13th Australasian Fluid Mechanics Conference
Monash University, Melbourne, Australia
13-18 December 1998

CROSS-STREAM OSCILLATIONS OF A CYLINDER ADJACENT TO A FREE-SURFACE: FLOW PATTERNS AND LOADING

J. Carberry[1], **J. Sheridan**[1], **J.-C. Lin**[2] **and D. Rockwell**[2]

1. Department of Mechanical Engineering
Monash University, Clayton, Victoria, AUSTRALIA

2. Department of Mechanical Engineering and Mechanics
Lehigh University, Bethlehem, PA, US

ABSTRACT

A technique of high-image-density particle image velocimetry and a method for simultaneous force measurement reveal the mechanisms leading to remarkable changes in the lift force on an oscillating cylinder, located both well below and adjacent to a free-surface. Patterns of instantaneous vorticity are related to the instantaneous lift; this approach defines the distinctive features of the near-wake and cylinder loading due to proximity of the free-surface.

INTRODUCTION

The flow patterns due to a cylinder oscillating in the cross-stream (transverse) direction, in absence of free-surface effects, have been extensively studied in recent years. The nature of the near-wake vortex patterns have been characterized primarily on a qualitative basis. A summary of previous related investigations, along with a preliminary study of the instantaneous, quantitative structure of the near-wake, are provided by Sheridan *et al.* (1998).

Little is understood of the effect of Reynolds number on the near-wake of an oscillating cylinder, especially in the range of Re = 1,000 to 3,000, for which the vortex formation length from the corresponding stationary cylinder becomes relatively long, as characterized by Lin *et al.* (1995). The issue arises as to whether oscillations of the cylinder in this range of Reynolds numbers promote a dramatic reduction in formation length, thereby potentially influencing the loading on the cylinder. Even at values of Reynolds number outside this range, for example, at Re = 185 and 5000, as addressed by Gu *et al.* (1994), reductions in the vortex formation length are detectable when the cylinder is subjected to low amplitude oscillations. In essence, at a constant value of excitation amplitude, a decrease in formation length is evident when the excitation frequency increases.

A further consideration of practical importance is the effect of an adjacent free surface on the vortex formation from, and loading on, a circular cylinder. Sheridan *et al.* 1997) have addressed the limiting case of flow past a stationary cylinder located immediately beneath a free surface; moreover, they summarize related investigations, including the case of a cylinder piercing the free-surface (Lin *et al.* 1996).

The present investigation focuses on quantitative imaging and force measurements for the case of cross-stream oscillations of a cylinder located well beneath and immediately adjacent to a free-surface. The instantaneous loading on the cylinder is related to instantaneous patterns of vortex formation and development of the near-wake region.

EXPERIMENTAL SYSTEM

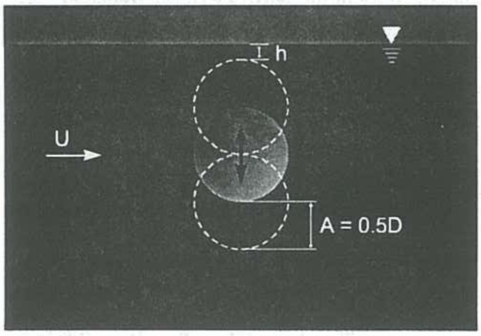

Figure 1 Schematic of oscillating cylinder.

The experiments were performed in a water channel in the Lehigh University fluid Mechanics Laboratories. The experimental system and approaches are described by Lin & Rockwell (1996). These experiments used a perspex cylinder which was 317 mm long, with a diameter D of 25.4 mm and was fitted with 368 mm diameter end plates. The free stream velocity U gives a Reynolds number of 2100 for the stationary cylinder where Re = UD/υ is based on the diameter of the cylinder. The cylinder was oscillated transverse to the free stream such that its vertical displacement is described by $y = A \sin 2\pi (f_e\ t)$, as shown in Figure 1. The amplitude ratio, $A/D = 0.5$ in all cases and the frequency ratio f_e/f_o was varied from 0.7 to 1.2 where f_o is the Strouhal frequency. The vertical distance from the top of the oscillation to the free-surface is h. The first experiment was performed with the cylinder located at half height in a water depth of 530 mm. The effect of the free-surface is negligible and the cylinder is considered to be fully submerged. The second experiment addressed the effect of the free-surface. The water depth was 352 mm and the cylinder was placed at $h/D = 3/16$. The forces on the cylinder were measured using a sting strain gauge system. Quantitative visualization involved a laser-scanning technique of high-image-density particle image velocimetry, described by Rockwell *et al.* (1993). The grid scale resolution of the velocity field obtained using high-image-density PIV was 3.9 x 3.9 mm for the submerged experiment and 2.8 x 2.8 mm for the surface experiment.

RESULTS AND DISCUSSION

Fully submerged cylinder

At frequencies above fe/fo = 0.7, the dominant frequency of the lift force is the frequency of oscillation, f_e and the amplitude of the lift coefficient, C_L, is small with a value of less then 1. As f_e, is increased we observe a large jump in the lift force, which increases by a magnitude of 3; the drag force increases only slightly. These features are evident in the quasi-steady response at fixed values of excitation frequency, fe/fo. In essence, one may view the abrupt increase in lift coefficient as a type of transition. Transition here implies the transformation between distinct states of the near wake: it is not related to laminar-turbulent transition. Frequencies at which transition occur are termed transition frequencies. For frequencies below transition the amplitude of the lift trace remains small apparently indefinitely. Disturbing the flow can induce large amplitude lift but this phenomena appears to be sustainable only in the presence of the transient. After a period of time the input flow returns to a steady state and the small amplitude lift trace returns.

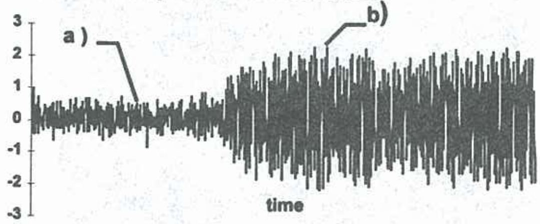

Figure 2 Time variation of lift coefficient $C_L=2L/\rho U^2 Dl$ showing transition from small to large lift for the submerged cylinder, frequency ratio, $f_e/f_o = 0.93$. Where L is the lift force on the cylinder, l is the cylinders length and ρ is the density of water.

This transition can also be observed during a single run when the cylinder is oscillating at a fixed frequency. For frequencies within the transition region, as illustrated in Figure 2, the lift is small after startup and has the same characteristics observed at the lower frequencies. After a period of time the lift amplitude becomes large with the transition occurring over a number of cycles. For the case of the submerged cylinder the (unforced) transition to large lift appears to be non-reversible. Again transition can be forced by disturbing the flow; however when the disturbance dies out the lift remains large.

At frequencies above transition the lift force becomes large immediately after startup. The amplitude of the lift increases with frequency.

Differences in the nature of the small and large lift traces are clearly demonstrated by their spectral content. The spectra in Figure 3 were calculated by breaking the lift trace shown in Figure 2 into small and large amplitude regions marked a) and b) respectively. The small lift trace gives a relatively strong peak at the frequency of oscillation but there is also significant energy at a band of frequencies just above this frequency. This broadband peak which appears to be centred at the natural, Karman shedding frequency of the (oscillating) system, is significant at lower frequencies of oscillation. As the frequency is increased towards the value at which transition occurs, the peak at f_e moves closer to this broad band peak. After transition, the peak at f_e is much stronger.

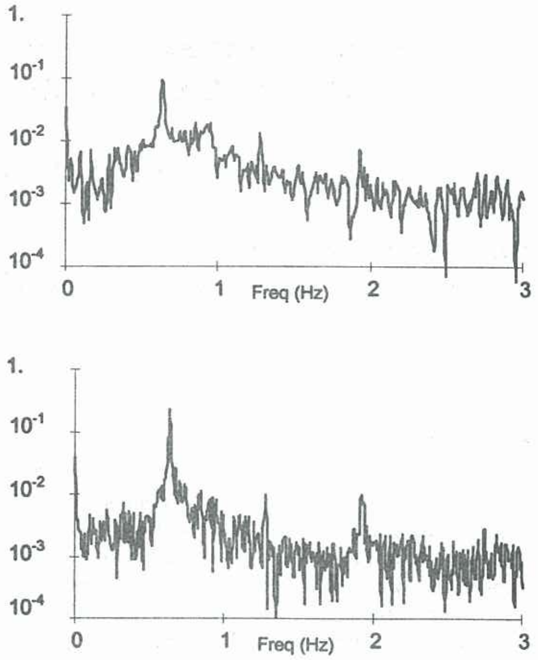

Figure 3 Lift spectra calculated using the segments of the lift trace, corresponding to **a)** small lift calculated using 1024 points, **b)** large lift calculated using 2048 points. Frequency ratio, $f_e/f_o = 0.93$.

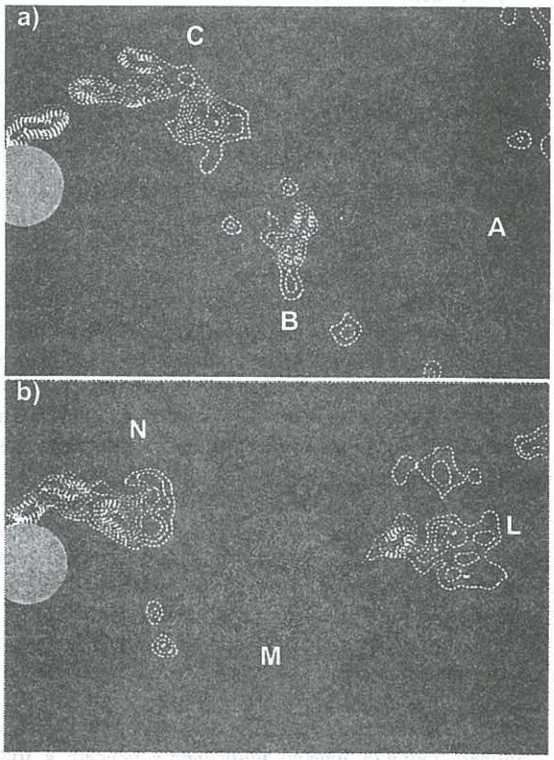

Figure 4 Instantaneous vorticity fields corresponding to **a)** small lift, **b)** large lift at the frequency ratio, f_e/f_o = 0.93, the cylinder is at the centre of its downwards motion in both cases. Positive (solid line) and negative (dashed line) vorticity contours have minimum and incremental values of $|\omega_{min}| = \pm 4$ sec^{-1} and $\Delta\omega = 4$ sec^{-1}.

The transition described above appears to involve a change in the mode of vortex shedding. Figure 4 shows images of the instantaneous vorticity fields occurring in the small and large amplitude regions of the lift trace marked a) and b) respectively in Figure 2. Figure 4a shows the small lift vortex shedding mode before transition. In this mode, two counter-rotating pairs are shed per oscillation in a similar fashion to the 2P mode described by the qualitative visualization of Williamson & Roshko (1988). One such pair is formed by the vortex structures marked A and B. As the cylinder approaches its lowest position the structure C will form a second pair with the positive vorticity concentration shed from the upper surface of the cylinder. A requirement of this mode of vortex shedding appears to be that the attached shear layers become long enough so that the same sign of vorticity can be shed into both the upper and lower wake. After transition, the vortex shedding mode produces two single vortices of opposite sign per oscillation. The vertical extent of the wake is much smaller than before transition. Thus, in Figure 4b, the shed vorticity over one cycle of oscillation is represented by structures N and M, whereas in Figure 4a, the vorticity shed in one cycle corresponds to the structures A, B, C and a portion of the positive vorticity adjacent to the cylinder. Comparing the development of vortex C before transition and N after transition, the large scale structure C has separated from the cylinder and appears to be more advanced. Thus, after transition, the large scale vortex structures appear to be shed from the cylinder slightly later in the cycle.

Throughout the range of frequencies studied, the shedding is observed to be symmetric about the centreline of the wake. The features described in the near-wake are repeatable and occur at the same frequency as the oscillation of the cylinder.

As the frequency of oscillation, f_e/f_o increases, a number of systematic changes were observed in the wake. The angle swept out during an oscillation by the instantaneous wake centre line increases. Also, the vortex structures form closer to the front stagnation point. The contraction of the wake can be observed by considering the distance from the front stagnation point at which the vortex structures are shed from the cylinder, or the vortex formation length. As the formation length becomes short, it is convenient to consider the positioning of a particular vortex structure at a given phase of the cylinder oscillation. See for example the positive vortex structure underneath the cylinder in Figure 6b and Figure 7b. The positioning of such structures depends upon both the formation length and the timing of shedding of vorticity from the cylinder. The transition described above appears to occur when the formation length decreases to a threshold value. This is similar to the limiting formation length at which Gu *et al* 1994 observed a switch in the initially formed vortex. In the images obtained by Gu *et al* it is also clear that the position of the vortex forming on the cylinder at a fixed phase contracts as the frequency, f_e/f_o increases. As the frequency of oscillation, f_e/f_o increases, the shedding of vorticity occurs later in the oscillation. The changes in the phase of the lift with respect to the displacement are consistent with changes observed in the timing of the vortex shedding in the oscillation cycle.

Cylinder oscillating underneath a free-surface

In order to investigate the effect of an adjacent free-surface, the cylinder is located at $h/D = 3/16$ (see Figure 1). As the frequency of oscillation is increased, we observe a transition similar to that observed for the fully submerged cylinder. There are, however a number of significant differences. Transition occurs at lower frequencies f_e/f_o and the increase in amplitude of the lift force at transition, as shown in Figure 5, is not as large. Also within the transition region it is possible for the lift to oscillate between the small and large amplitude states. Thus in Figure 5 we observe the return of the small lift amplitude after the initial transition. This reversal of transition was never observed for the fully submerged cylinder.

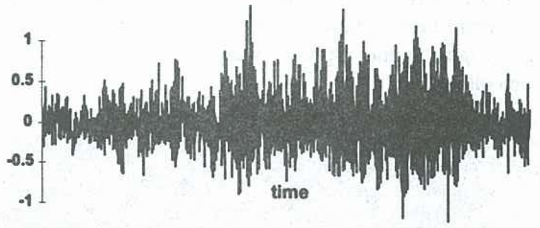

Figure 5 Time variation of lift coefficient, $C_L=2L/\rho U^2 Dl$ for the cylinder near the free-surface $h/D = 3/16$, showing intermittent transition from small to large lift, frequency ratio, $f_e/f_o = 0.84$.

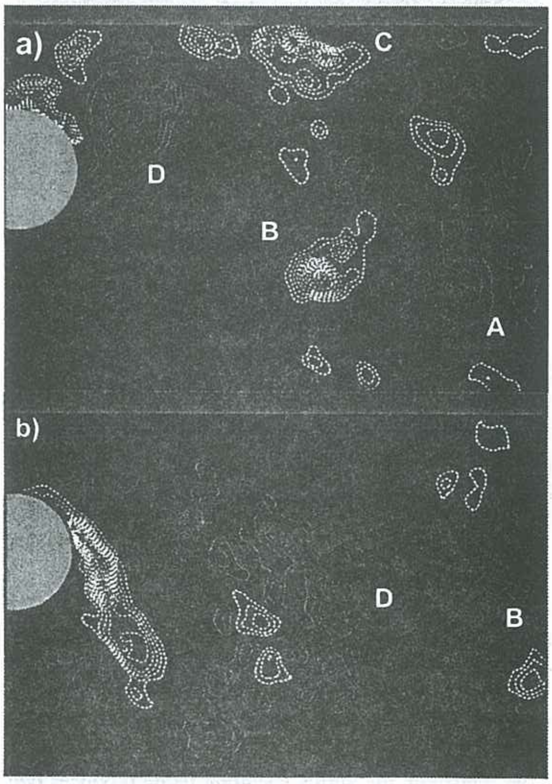

Figure 6 Instantaneous vorticity field corresponding to small amplitude lift for the cylinder near the free-surface, $h/D = 3/16$. The cylinder is shown at the midpoint of its **a)** downward and **b)** upward motion. Frequency ratio, $f_e/f_o = 0.83$. Positive (solid line) and negative (dashed line) vorticity contours have minimum and incremental values of $\omega_{min} = \pm 5$ sec^{-1} and $\Delta\omega = 5$ sec^{-1}.

In order to illustrate the key features of the transition, cases of steady-state response are considered before and after transition. The vorticity fields shown in Figure 6 and Figure 7 are for slightly different frequencies and demonstrate the differences between large and small lift. Prior to transition, Figure 6 shows the generation of a counter-rotating vortex pair A, B, and a single vortex structure C in each cycle. The shedding of negative vorticity occurs just after the top of the oscillation cycle where the negative vortex structures marked B and C are shed into the lower and upper wake respectively. The structure D is analogous to A which was shed one cycle earlier. The single shedding of positive vorticity, D (or A) is shed into the middle of the wake and moves downwards slightly to form a pair with the negative vorticity shed into the lower wake. The shedding is markedly anti-symmetric. If the shedding were symmetric about the centre line of the wake then the images a) and b) in both Figure 6 and Figure 7 would be mirror images of each other.

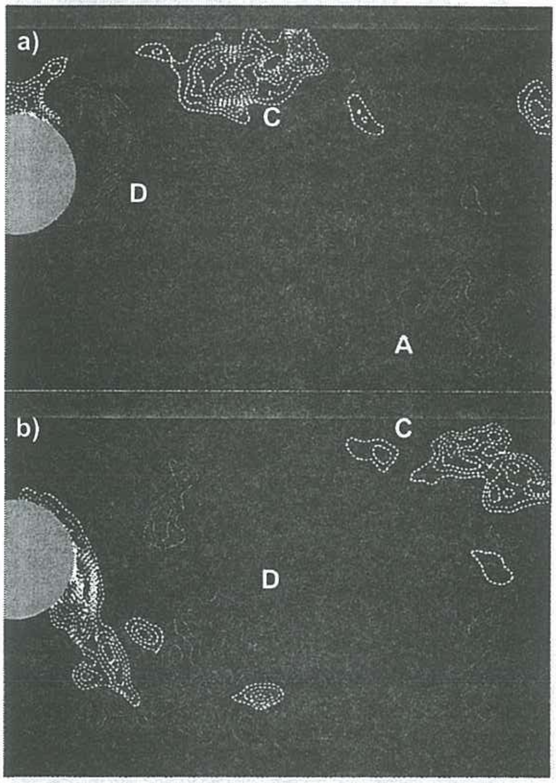

Figure 7 Instantaneous vorticity field corresponding to large amplitude lift for the cylinder near the free-surface, h/D = 3/16. The cylinder is shown at the mid point of its **a)** downward and **b)** upward motion. Frequency ratio, $f_e/f_0 = 0.85$. Positive (solid line) and negative (dashed line) vorticity contours have minimum and incremental values of $\omega_{min} = \pm 5\ \text{sec}^{-1}$ and $\Delta\omega = 5\ \text{sec}^{-1}$.

After transition, the vortex shedding mode produces two single vortices of opposite sign as shown in Figure 7. The shedding is slightly anti-symmetric as the vortex shed upwards is constrained by the surface. It is interesting to note that, after transition, the vortex structures demonstrate a greater degree of symmetry about the centre-line of the wake then before transition. By comparing the relative positions of the lower vortex A in Figure 7a and the upper vortex C in Figure 7b we observe that the vortex structure under the surface has traveled slightly further away from the cylinder. As for the submerged case, the shedding events occur slightly later in the cycle after transition. This is clear if we compare the progress of the vortex structures C in Figure 6 (small lift, before transition) with their corresponding structure C Figure 7 (large lift, after transition). As for the submerged case there is also a clear decrease in the vortex formation length accompanying the transition from small to large lift.

CONCLUSIONS

By increasing the frequency of oscillation, a remarkable increase in the amplitude of the lift force on the cylinder has been observed for both a fully submerged cylinder and a cylinder just under a free-surface. In both these cases, the increase in the lift force was found to correspond to a change in the mode of vortex shedding. However, when the cylinder was in close proximity to the free-surface the increase in the lift force was less then that for the fully-submerged cylinder.

The role of vortex formation length and the timing of events in the near wake appear to be important in understanding the dramatic changes observed with transition. Transition appears to be linked with the contraction of the wake to a threshold point, similar to that observed by Gu *et al* 1994. Comparing the case where the cylinder is in close proximity to the free-surface with the fully submerged case, we observe that the shedding events occur much later for the submerged case. This is consistent with the phase of the lift recorded for both cases.

REFERENCES

GU, W., CHYU & ROCKWELL, D. "Timing of vortex formation from an oscillating cylinder", *Physics of Fluids* **6**, 3677-3682, 1994.

LIN, J.-C., & ROCKWELL, D. "Experimental Data for Computational Fluid Dynamics Simulation of Fluid Oscillators: Cavity Flow. Volumes I and II", Fluid Mechanics Laboratories Report R01, Department of Mechanical Engineering and Mechanics, Lehigh University, 1996.

LIN, J.-C., SHERIDAN, J. and ROCKWELL, D. "Near-Wake of a Perturbed, Horizontal Cylinder at a Free-Surface", Physics of Fluids, 8 (8), 2107-2116, 1996.

LIN, J.-C., TOWFIGHI, J. and ROCKWELL, D. "Instantaneous Structure of Near-Wake of a Circular Cylinder: On the Effect of Reynolds Number", Journal of Fluids and Structures, 9, 409-418, 1995.

ROCKWELL, D. MAGNESS, C., TOWFIGHI, J., AKIN, O., and T. CORCORAN "High Image-Density Particle Image Velocimetry Using Laser Scanning Techniques", Experiments in Fluids, 14, 181-192, 1993

SHERIDAN, J., CARBERRY, J., LIN, J.-C. & ROCKWELL, D. "On the near-wake topology of an oscillating cylinder", *Journal of Fluids and Structures*, 1998 (in press).

SHERIDAN, J., LIN, J.-C. & ROCKWELL, D. "Flow past a cylinder close to a free-surface", *Journal of Fluid Mechanics* **330**, 1-30, 1997.

WILLIAMSON, C.H.K. & ROSHKO, A. "Vortex formation in the wake of an oscillating cylinder", *Journal of Fluids and Structures* **2**, 355-381, 1988.